Structural Chemistry
https://doi.org/10.1007/s11224-026-02754-0

RESEARCH

Is QTAIM compatible with resonance? an investigation using eigenvectors and eigenvalues of LDMs

James S. M. Anderson[1]

Received: 1 December 2025 / Accepted: 15 February 2026

Abstract
The eigenvalues and eigenvectors of the Localization-Delocalization Matrices (LDMs) are interpreted and computed for molecular examples. It is found that eigenvectors corresponding to the largest eigenvalues reflect the intuitive pictures of molecules, functional groups, and resonance structures. The eigenvectors can each be thought of as a collective direction of the flow of electrons between atoms. Localization modes and delocalization modes are introduced where the localization modes can be interpreted to define functional groups and delocalization modes can be interpreted as resonance structures and quantify the number of electrons netted from each flow. The eigenvalues and eigenvectors are found to be related to those of the negative of the inverse of the hardness matrix, the negative of the softness matrix, suggesting the eigenvectors associated with the largest eigenvalues are patterns of restricted electron flow and the suggesting the eigenvectors associated the smallest positive eigenvalues are patterns of free electron flow.

Keywords Localization-delocalization matrix · LDM · Quantum theory of atoms in molecules · QTAIM · Hardness matrix inverse · Softness matrix

Introduction

A concept that is ubiquitous in predicting chemistry is that of resonance structures [1–5], but this concept tends to be elusive from a quantum mechanical perspective [6]. Resonance can be described as the idea that electrons can delocalize over several atoms forming short-lived bonds or localizing to an atom. Resonance structures primarily involve π electrons (those found in double or triple bonds). In the language of resonance structures, these bonds or localizations tend to occur at particular atoms. That is, an atom will form different numbers of bonds with its neighbours that it has a sigma bond with or an atom will absorb the electrons being transferred [1]. Resonance diagrams have been helpful in predicting reactivity [1–5]. However, resonance is a fuzzy concept at best. In fact, Levine's Quantum Chemistry text books states "resonance is not a real phenomenon." [6] The concept was developed in terms of valence bond theory and is also related to Hückel theory [6]. The sharing concept can be thought of as an electron delocalization concept.

The Quantum Theory of Atoms In Molecules (QTAIM) is a method that discerns the properties of atoms within a molecule within a quantum mechanical framework [7–11]. The most obvious quantity that is computed is atomic charge, but virtually any other measureable property that can be computed for an entire molecule can also be computed for an atom within the molecule using this method. Resonance is often thought of being at odds with the Quantum Theory of Atoms In Molecules since it is not readily measurable [6]. However, there is a branch of QTAIM that captures the concept of localization and delocalization of electrons [7, 8, 12–14]. This branch is the most obvious to make a connection with the topic of resonance as resonance is related through the delocalization of primarily π electrons. Bader and Stephens [13] introduced a measure for the number of localized electrons an atom has and a measure for the number of electrons shared between a pair of atoms, delocalized electrons. They introduced these concepts through Localization Indices and Delocalization Indices (LIs and DIs respectively). Matta in 2014 [15, 16] introduced the concept of the Localization-Delocalization matrices (LDM

✉ James S. M. Anderson
james.anderson@iquimica.unam.mx

[1] Instituto de Química, Universidad Nacional Autónoma de México, Universidad 300, Ciudad Universitaria, Ciudad de México 04510, México

Published online: 05 May 2026

or ζ). These matrices arrange the LIs on the diagonal and half of the values of the DIs are on the off-diagonals. The localization index can be interpreted as the measure of the electrons associated with an atom that are not shared with other atoms. In the case where the localization index of an atom is nearly equal to the population implies the atom is may be involved in ionic bonding or no bonding at all [13, 17]. The delocalization index can be interpreted as the number of electrons shared between two atoms and has been used as a measure of bond order [8, 18].

The LDM is a logical extension of the LI and DI concept and has been used in a variety of applications [14, 15, 19–39]. These matrices can be generated using the software created by Sumar et al. [35] that reads an AIMALL [36] output file. The LDMs have been used in many contexts. Sumar et al. used the eigenvalues and the Frobenius distances of the LDMs and submatrices of the LDM to assess relative aromaticity [37]. Another context where LDMs have been used is with principle component analysis to build predictive models of the toxicities of semiochemicals to mosquitos combining the electroantennographic responses to the repellents [38]. One other application is that the LDM and submatrices of the LDM have been applied to predict pKa's and UV-wavelengths (ultraviolet-wavelengths) of maximum absorbance with high correlation [24, 39]. Most of the work carried out with the LDM concept involves using submatrices of the LDM and comparing the Frobenius norms of chemical systems. The approach detailed here involves using the eigenvectors and eigenvalues of the LDM to identify the molecule or molecules within a given chemical system. Then within the identified molecules determine the functional groups identifying the resonance structures. This paper is laid out as follows. Section II is the theoretical development where QTAIM, LI, DI, LDM and how the associated eigenvalues and eigenvectors are used to determine the molecules, functional groups, and resonance structures. Section III contains the results, and Section IV contains the conclusions.

Theoretical development

The Quantum Theory of Atoms In Molecules (QTAIM) is a powerful method for the discerning atomic properties for the atoms within a molecule [7–11]. It is a vast and rich field where details are described in the literature. Here only concepts used in this article are described. In QTAIM an atom is a nonoverlapping volume of electron density, Ω. The boundary of the atoms within a molecule are defined by the zero-flux condition where the flux of the density vanishes,

$$\int_{\Omega} \nabla^2 \rho(\boldsymbol{r}) d\boldsymbol{r} = 0 \tag{1}$$

where $\rho(\boldsymbol{r})$ is the electron density and ∇^2 is the Laplacian. This is the more general condition [7, 9, 40–42]. Typically, a sufficient condition that satisfies Eq. (1) is used

$$\nabla \rho(\boldsymbol{r}) \cdot \boldsymbol{n} = 0 \tag{2}$$

where ∇ is the gradient and $\boldsymbol{n}$ is the normal to the surface of Ω. Bader and coworkers argued these zero-flux conditions follow from the Schwinger principle of stationary action applied to a volume. Their treatment found that only a volume with a boundary that satisfies Eq. (1) is satisfactory [7, 9, 40]. The treatment has been extended into relativistic considerations where the same boundary condition in Eq. (1) or Eq. (2) is left unchanged though in some cases more boundaries are allowable [43–47]. In passing, for completeness, it is pointed out that there is some controversy with this treatment, but it will be overlooked here [48–56]. Generally an atom is defined by selecting a volume that satisfies Eq. (2) that contains a maximum within the volume, which is the case in this work [7]. There is some work that explores where the maxima are included on the boundary instead of within the atom [57–62]. These volumes with a single maximum within the atom are often called basins. Typically these maxima are associated with a nucleus, though occasionally maxima occur elsewhere known as nonnuclear maxima [7, 9, 63, 64]. In this typical formulation of the boundary of the atoms there are critical points lying on the boundary. Critical points are points where the gradient of the density is zero. These include bond critical points, ring critical points and cage critical points. A bond critical point is a saddle point in the electron density with two negative curvatures and one positive curvature. A ring critical point is a saddle point in the electron density with one negative curvature and two positive curvatures. Cage critical points are minima in the electron density. These critical points are useful in identifying and chemical phenomena such as bonding. More detail can be found in the literature [7–11].

Most QTAIM properties are formulated as above. The localization and delocalization indices [7, 8, 12–14] are formulated over two basins. The localization index for atom A is defined as (with the common notations included)

$$\begin{aligned} &\mathrm{LI}(A) = \Lambda(A) = \Lambda(\Omega_A) = \lambda(A) = \Lambda(A) \\ &= \lambda(\Omega_A) = \int_{\Omega_A} \int_{\Omega_A} \rho_{xc}(r_1, r_2) dr_1 dr_2 \end{aligned} \tag{3}$$

and the delocalization index between atoms A and B is defined as (with the common notations included)

$$\mathrm{DI}(A,B) = \delta(A,B) = \delta(\Omega_A,\Omega_B) = 2\int_{\Omega_A}\int_{\Omega_B}\rho_{xc}(\boldsymbol{r}_1,\boldsymbol{r}_2)d\boldsymbol{r}_1 d\boldsymbol{r}_2 \tag{4}$$

where $\rho_{xc}(\boldsymbol{r}_1,\boldsymbol{r}_2)$ is the exchange-correlation pair-density, which is defined here as

$$\rho_{xc}(\boldsymbol{r}_1,\boldsymbol{r}_2) = \rho(\boldsymbol{r}_1)\rho(\boldsymbol{r}_2) - \rho_2(\boldsymbol{r}_1,\boldsymbol{r}_2) \tag{5}$$

that depends on the pair-density $\rho_2(\boldsymbol{r}_1,\boldsymbol{r}_2)$. Note that sometimes the exchange-correlation pair density is defined with the opposite sign [65].

The elements of the LDM matrix, LDM_{ij}, are defined as

$$\mathrm{LDM}_{ij} = \zeta_{ij} = \begin{cases}\lambda(\Omega_{ii}) & i = j\\ \delta(\Omega_i,\Omega_j)/2 & i \neq j\end{cases} \tag{6}$$

An important relationship is that the population of atom i is equal to the sum of the elements of the i^{th} row (or column),

$$\sum_j \zeta_{ij} = N(\Omega_i) = \sum_j \zeta_{ji} \tag{7}$$

where $N(\Omega_i)$ is the population of atom i, the number of electrons that belong to atom i

$$N(\Omega_i) = \int_{\Omega_i}\rho(\boldsymbol{r})d\boldsymbol{r} \tag{8}$$

Likewise, the sum over all the elements of the LDM yields the number of electrons of the molecule

$$\sum_{ij}\zeta_{ij} = \sum_i N(\Omega_i) = N \tag{9}$$

that is also recovered by the relation

$$\int \rho(\boldsymbol{r})d\boldsymbol{r} = N \tag{10}$$

where N is the total number of electrons in the chemical system [16].

To understand the LDM better it is worth making analogy to a more established related construction, namely the hardness matrix [66–76]. The LDM captures the idea of electron flow. This is argued by through the localization indices, immobility of electron movement, and delocalization indices, mobility of electrons between atom pairs. The LDM is not directly an energy construction, but electron populations in real space are determined by the energy. The hardness matrix is a Hessian of the change of energy with respect to atomic charge or population [66–77]. Explicitly the elements of the hardness matrix, η_{ij}, in terms of electron population can be written as

$$\eta_{ij} = \frac{\partial E(N(\Omega_1),\ldots,N(\Omega_n))}{\partial N(\Omega_i)\,\partial N(\Omega_j)} \tag{11}$$

noting that the typical form is in terms of atomic charge instead of atomic electron population as written here. Though the LDM is not explicitly a Hessian the relationship between the elements the LDM and the hardness matrix allows this interpretation. The i^{th} diagonal element of the hardness matrix is the resistance of atom i in changing its electron population and the i,j^{th} off-diagonal element of the hardness matrix represents the charge coupling between atoms i and j. The harder an atom is the more localized the electrons are, and the higher cost to change in electron population leading to larger diagonal suggesting a larger LI. The more shared electrons the stronger the coupling of electrons resulting in larger off-diagonal elements in magnitude. Therefore, the larger the eigenvalue the more resistant to electron flow, related to steeper curvature. This can be interpreted as the larger the eigenvalue the more likely an electron will stay at an atom within that electron flow as described by the eigenvector. Thus, the eigenvectors associated with larger eigenvalues can be interpreted as electron flow that changes slowly. As such, the eigenvectors associated with localized modes are the familiar functional groups, electrons stay within that group and, particularly, at those atoms. This also extends to the eigenvectors associated with delocalization modes where larger eigenvalues can be interpreted as stabilizing different resonance configurations. In other words, the larger eigenvalues associated with the delocalization modes allows for the accumulation of charge on a single atom before transferred. As the eigenvalues get smaller the electrons in the associated eigenvectors move more freely through the pattern and the structures become more averaged. The approximate relationship between the LDM and the hardness matrix along with an interpretation in the role the eigenvalues play in the total energy is given in Appendix A. Summarizing here the approximate relationship between the LDM and the hardness matrix, the LDM is approximately proportional to the negative of the inverse of the of the hardness matrix. This means that the LDM and the hardness matrix have approximately the same eigenvectors and the eigenvalues of the LDM are generally correlated with the eigenvalues of the hardness matrix through being approximately proportional to the negative reciprocal with each other. Note that the inverse of the hardness matrix is often called the softness matrix, but there are other related matrices referred to as the softness matrix [76].

In addition to the eigenvalues being interpreted as curvature, the larger an eigenvalue is the less sensitive is to changing by the addition of a small perturbing matrix. There is a result by Weyl that gives bounds on the eigenvalues of a symmetric matrix like LDM and a perturbing matrix. He

showed that the eigenvalues of the resulting matrix has the eigenvalues of the LDM that vary by no more in an absolute difference sense than the absolute maximum eigenvalue of the perturbing matrix [78]. The eigenvectors tend to be affected most by the eigenvectors with the same or nearly the same eigenvalue. The maximum an eigenvector is rotated is found through the Davis-Kahan sine theorem [79]. Both Weyl's result and Davis-Kahan's result can be argued from perturbation theory [6]. This gives the interpretation that the resistance to electron flow within a pattern is insensitive to a small perturbation, but a pattern may merge with those with patterns with similar eigenvalues upon perturbation.

Another view from the hardness matrix is in its role with a small perturbation in the energy. At first order this preferentially activates the eigenvectors associated with the smallest eigenvalues. This confirms the interpretation that the smaller eigenvalue modes allow for easier flow of the electrons, see Appendix A.

The eigenvalues, λ_is, will be referred to as localization constants. Though the eigenvalues have units of number of electrons they are not the number electrons associated with the mode. The sum of the eigenvalues is equal to the number of localized electrons,

$$\sum_i \Lambda\left(\Omega_i\right) = \sum_i \lambda_i \tag{12}$$

A more practical measure is in terms of the vector

$$\boldsymbol{v}_k = \left(\lambda_k \sum_j \xi_{j,k}\right) \boldsymbol{\xi}_k \tag{13}$$

where $\xi_{j,k}$ is the j^{th} element of the eigenvector $\boldsymbol{\xi}_k$ that is associated with the localization constant λ_k. This has the property that summing over all $\boldsymbol{v}_k$ yields the population of each atom,

$$\sum_k \boldsymbol{v}_k = \begin{bmatrix} N\left(\Omega_1\right) \\ N\left(\Omega_2\right) \\ \vdots \\ N\left(\Omega_n\right) \end{bmatrix} \tag{14}$$

for all n atoms. The derivation is in Appendix B. Thus the elements of $\boldsymbol{v}_k$ can be interpreted as the final number of electrons (net) that the $\boldsymbol{v}_k$ mode deposits into each atom (they can be zero or negative). Notice that multiplying the eigenvector $\boldsymbol{\xi}_k$ by -1 (a phase) does not change the value of the elements of $\boldsymbol{v}_k$ due to $\boldsymbol{v}_k$'s quadratic dependence on the elements of the eigenvectors $\boldsymbol{\xi}_k$. Also notice that the sum over the vectors $\boldsymbol{v}_k$, Eq. (14), and then summing over all the elements of this sum yields the total number of electrons. From Eq. (13) for non-zero eigenvalues the sign of each of the elements of $\boldsymbol{v}_k$ is the same using either $\boldsymbol{\xi}_k$ or $-\boldsymbol{\xi}_k$. It also follows that if the j^{th} element of $\boldsymbol{\xi}_k$ is 0 then the j^{th} element of $\boldsymbol{v}_k$ is also zero. This suggests choosing the eigenvectors of $\boldsymbol{\xi}_k$ so that the sign of the elements match that of $\boldsymbol{v}_k$. The advantage of this is it gives an interpretation of the direction of the electron delocalization flow using the signs of the elements of the eigenvectors. This leads to an interpretation of $\boldsymbol{\xi}_k$ and $-\boldsymbol{\xi}_k$. The elements of $\boldsymbol{\xi}_k$ with a positive sign will gain electrons while the elements with a negative sign will lose electrons. Since $-\boldsymbol{\xi}_k$ is also a valid eigenvector then the reverse happens. The corresponding $\boldsymbol{v}_k$ indicates whether $\boldsymbol{\xi}_k$ or $-\boldsymbol{\xi}_k$ is dominant in determining how many electrons will be netted at each atom.

Another point to consider is when the LDM is a block diagonal matrix (or nearly block diagonal) [6]. This would happen when an atom is (or atoms are) not exchanging or delocalizing electrons with other atoms. An interpretation is that each block defines a chemical system (different molecules).

For the LDM matrix (or each block) the eigenvectors have two main types.

1) Suppose the sign of the elements of the eigenvector match for several atoms and the remaining atoms are zero or near zero with correspondingly large values of the elements of$\boldsymbol{v}_k$ (around the value of the corresponding localization index values or even the population of the atom). The atoms that correspond to the large elements of the corresponding eigenvectors and $\boldsymbol{v}_k$ can often be interpreted as functional groups of the molecule. These are termed localization modes.

2) Suppose the sign of the elements of the eigenvectors mismatch and the absolute values of the elements of $\boldsymbol{v}_k$ are less than 2 but positive (or zero). These eigenvectors can be interpreted as a resonance structure particularly when the sum of the elements of the vector $\boldsymbol{v}_k$ or $\boldsymbol{\xi}_k$ is zero (or near zero). This allows for both signs of $\boldsymbol{\xi}_k$ and $-\boldsymbol{\xi}_k$ to be a resonance mode. These are termed delocalization modes. The value 2 is chosen pragmatically. It is taken because most atoms in most chemical systems, other than the hydrogen atoms, will generally have more than 2 localized electrons.

Summing over localization modes (within a Jordan block (block diagonal) [6] or all localization modes) yields a vector that closely resembles the localized electrons or population. This can be used to find the prominent localized mode to exchange electrons with the delocalization modes. This can be interpreted as a base resonance structure and the other resonance structures can be constructed from this.

Degenerate eigenvalues are likely to appear in symmetric systems. For delocalization modes each linear combination can be interpreted as a valid resonance structure. For localization modes they will often correspond to equivalent

groups and, for interpretation purposes, it is expected to be best to choose the set of localization modes from the degenerate modes that capture the functional groups separately.

As mentioned above and in Appendix A, the larger the eigenvalue the more prominent/stable/resistant to electron flow the corresponding mode is. In most cases the eigenvalues will be positive. Eigenvalues with value zero will correspond to a delocalization mode, and is expected to be one that has no impact on the atoms not participating. The electrons within this mode will move freely without barrier. This will always yield a $\boldsymbol{v}_k$ that is the zero vector. Negative eigenvalues are expected to be even rarer for the LDMs. These can be interpreted as weak modes that are unstable as electrons are expected to vacate the mode due to the negative curvature. These negative eigenvalues will typically be small in magnitude, and, by Weyl's theorem [78], a small perturbation to the LDM is likely to remove nonpositive eigenvalues.

Computational methods

All calculations were carried out using Kohn-Sham Density-Functional Theory (DFT) [80–83] using the ωB97X-V functional [84–86] and the 6-311++G** [87–89] basis set as implemented in the ORCA 6.1.0 where the Kohn-Sham orbitals are computed [90–96]. For the QTAIM properties including the LIs and DIs were computeds with AIMALL 19.10.12 Professional [36]. Eigenvalues and eigenvectors of LDM were computed with in-house software. For 4-bromonitrobenzene the scalar relativistic zeroth order regular approximation (SR-ZORA) was used for relativistic corrections [44–46, 97–105].

Results and discussion

Three representative molecules were considered. The first is acetic acid, see Fig. 1, that has been examined with LDM theory [16, 19]. The second is 4-bromonitrobenzene chosen, see Fig. 2, because it contains multiple distinctive groups (functional groups); it contains benzene, bromine, and nitro groups. Finally, 10-hydroxy-10,9-borazarophenanthrene that that contains a 1,2-azaborene group [106] with a hydroxyl group bonded to the boron group in a phenanthrene formation with 1,2-azaborene as the middle ring was chosen, see Fig. 3 [107]. This molecule and several chemical derivatives are known for having unusual reactivity [108, 109]. In fact, it was this unusual reactivity that was the motivation for the development of the General-Purpose Reactivity Indicators (GPRI) [109–117] within the conceptual DFT framework [66, 118] to explain its reactivity. Ureiro-Cueto and Anderson also considered this treatment for TiO_2 rutile in a separate article [119].

Acetic acid

Briefly, a summary of what the tables show is given. Tables 1, 2 and 3 are associated with acetic acid with the atoms listed as in Fig. 1. They all contain the corresponding population (number of electrons) and LI for each atom for convenience.

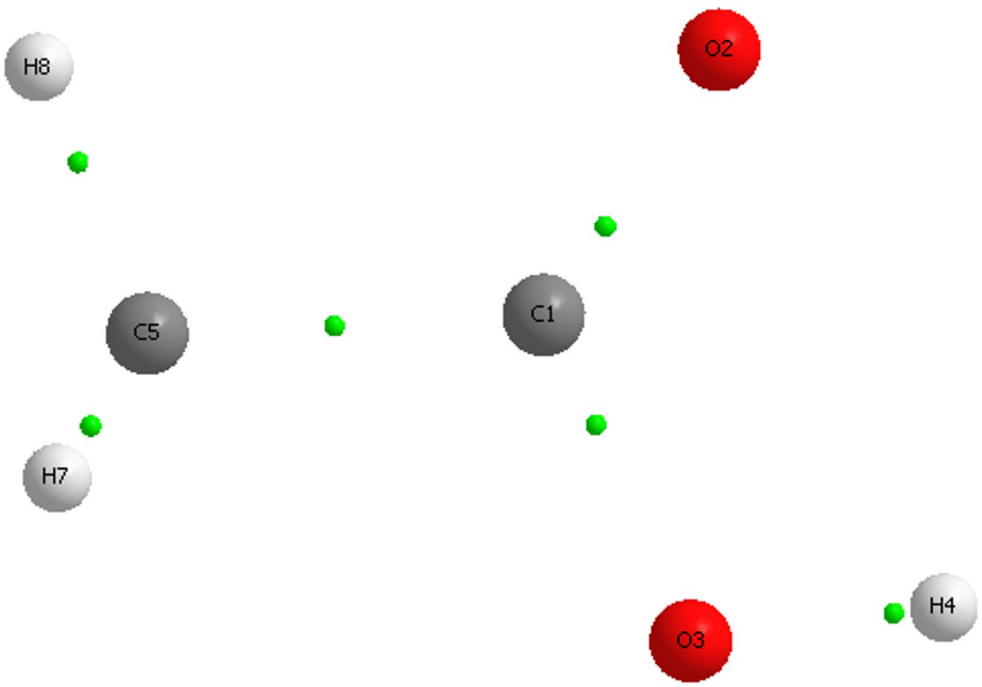

Fig. 1 Structure of acetic acid utilized. Large grey circles represent carbon atoms, large red circles represent oxygen atoms, and large white circles represent hydrogen atoms. The small green circles represent bond critical points. The symbols and numbers are used in tables to assign properties to each atom

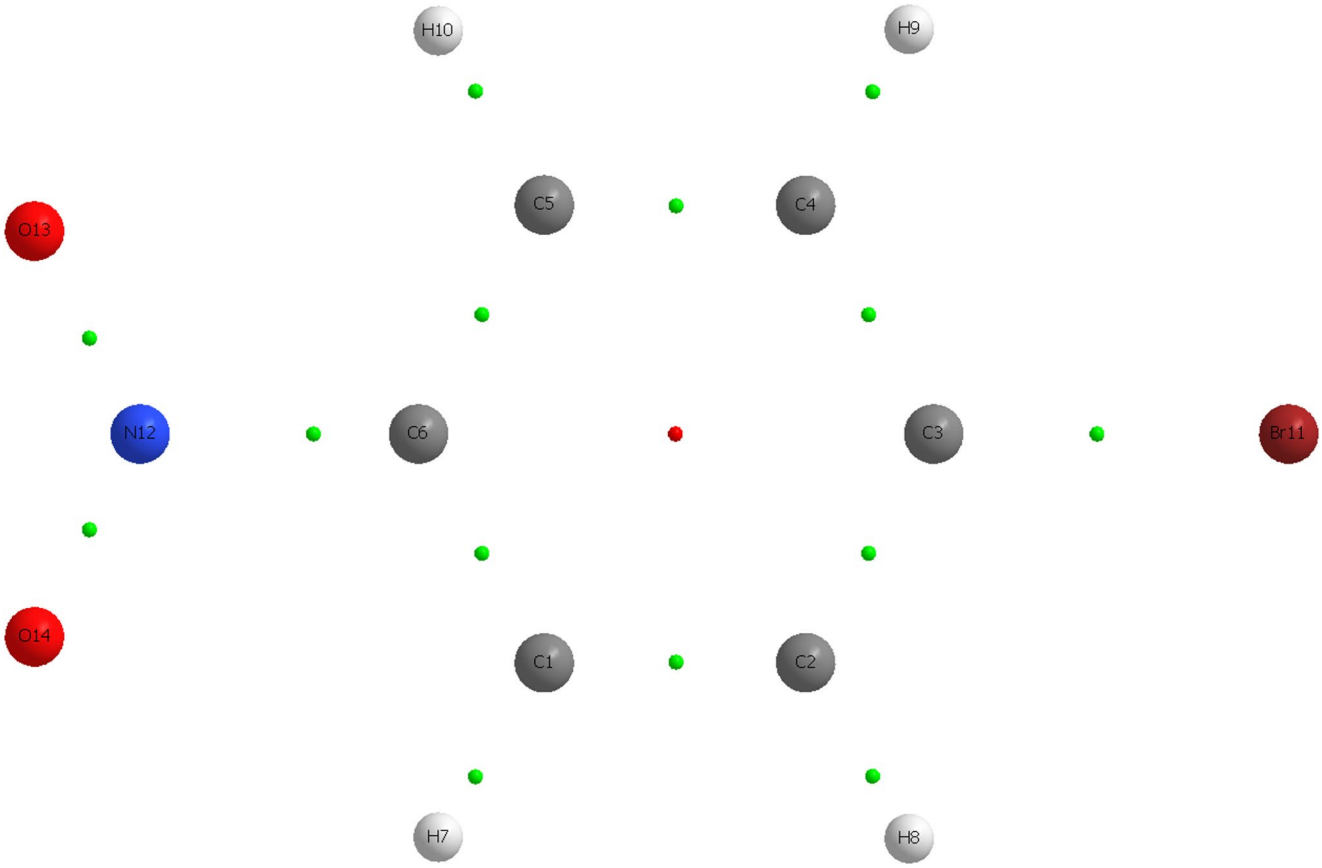

Fig. 2 Structure of 4-bromonitrobenzene utilized. Large grey circles represent carbon atoms, large red circles represent oxygen atoms, large blue circles represent nitrogen atoms, large brown atoms represent bromine atoms, and large white circles represent hydrogen atoms. The small green circles represent bond critical points, and the small red circles represent ring critical points. The symbols and numbers are used in tables to assign properties to each atom

- Table 1: associated with λ_1, and λ_3 are localization modes, and associated with λ_2 and λ_4 are delocalization modes.
- Table 2: associated with λ_8 is a localization mode, and associated with λ_5, λ_6, and λ_7 are all delocalization modes.
- Table 3: the sum of the localization modes.

Table 1 shows results associated with the 4 largest eigenvalues in decreasing order. The largest eigenvalue is 8.5072, approximately 1/3 of the total LI and the sum of the coefficients of $\boldsymbol{v}_1$ is 21.1 approximately 2/3 of the population. All of the elements of $\boldsymbol{v}_1$ are positive with none smaller than 10^{-2}. This suggests the molecule, but it is mainly defining the functional carboxylic acid with the two oxygens and the carboxylic acid hydrogen. The elements of $\boldsymbol{v}_1$ associated with O2 has 120% of its population (between an anion and dianion), with O3 has 82% of its population (approximately neutral), H4 has 72% of its population (nearly neutral), and C1 has 42%. This low inclusion of C1 is due to C1 playing a role in two functional groups, the carboxylic acid group, and the methyl group that appears in the localization mode $\boldsymbol{v}_1$. This suggests a mode similar to a resonance structure where the O2 has the electron that would be associated with a double bond between O2 and C1.

The second largest eigenvalue is 8.0731, approximately 1/3 of the total LI, but the sum of the elements of $\boldsymbol{v}_2$ is 0.707 approximately a single electron. Based on the elements of $\boldsymbol{v}_2$ associated with O2 and O3 that O2 is essentially transferring −1.34 electrons to O3. The net gain in O3 is 1.97 electrons.

The third largest eigenvalue is 4.28878, approximately 1/6 of the total LI, but the sum of the elements of $\boldsymbol{v}_3$ is 9.18 approximately that of the methyl group population (91% of the methyl group population) and a portion of the carboxylic acid carbon (38%). This is defining the mode associated with the methyl functional group containing some portion of the carboxylic acid carbon.

The fourth largest eigenvalue is 2.5873, approximately 1/8 of the total LI, but the sum of the elements of $\boldsymbol{v}_4$ is 3.43 approximately 1/3 of an electron. Based on the elements of $\boldsymbol{v}_2$ associated with O2 and O3 that O2 is essentially

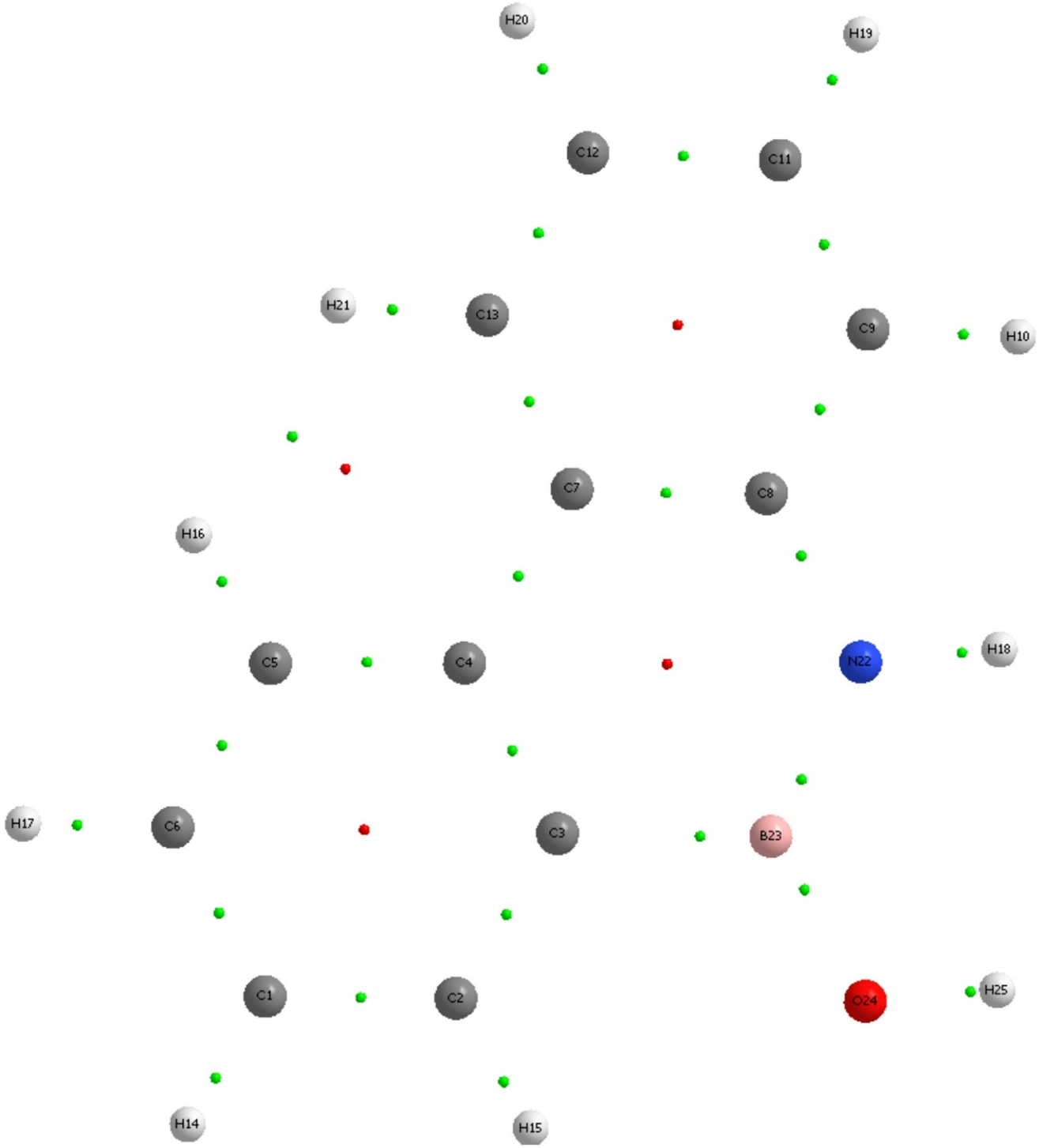

Fig. 3 Structure of 10-hydroxy-10,9-borazarophenanthrene utilized. Large grey circles represent carbon atoms, large red circles represent oxygen atoms, large blue circles represent nitrogen atoms, large pink circles represent boron atoms, and large white circles represent hydrogen atoms. The small green circles represent bond critical points, and the small red circles represent ring critical points. The symbols and numbers are used in tables to assign properties to each atom

Table 1 Acetic acid properties (see Fig. 1). The QTAIM number of electrons (population), localization index (LI), the first four largest eigenvalues, λ_i, listed in decreasing order, listed with the corresponding eigenvectors, and localization modes. Each mode is labelled if it is a localization mode (the absolute value of at least one element of $\boldsymbol{v}_k$ is greater than or equal to 2) or delocalization mode (otherwise) where significant elements are shown in yellow and black respectively

Atom	Population	LI	ξ_1	v_1	ξ_2	v_2	ξ_3	v_3	ξ_4	v_4
			λ_1=8.5072 Localized		λ_2=8.0731 Delocalized		λ_3=4.28878 Localized		λ_4=2.5873 Delocalized	
C1	4.43E+00	2.82E+00	1.37E-01	1.84E+00	-2.41E-03	-5.76E-03	2.68E-01	1.68E+00	9.53E-01	8.98E-01
O2	9.18E+00	8.29E+00	8.18E-01	1.10E+01	-5.62E-01	-1.34E+00	-5.57E-02	-3.49E-01	-1.04E-01	-9.77E-02
O3	9.12E+00	8.16E+00	5.57E-01	7.46E+00	8.26E-01	1.97E+00	-3.93E-02	-2.47E-01	-6.69E-02	-6.30E-02
H4	4.10E-01	7.32E-02	2.19E-02	2.94E-01	3.21E-02	7.66E-02	-1.72E-03	-1.08E-02	-7.10E-03	-6.69E-03
C5	5.98E+00	3.98E+00	3.13E-02	4.19E-01	1.92E-03	4.59E-03	9.39E-01	5.89E+00	-2.62E-01	-2.47E-01
H6	9.57E-01	4.10E-01	3.63E-03	4.87E-02	1.47E-04	3.50E-04	1.17E-01	7.35E-01	-4.89E-02	-4.61E-02
H7	9.57E-01	4.10E-01	3.63E-03	4.87E-02	1.47E-04	3.50E-04	1.17E-01	7.35E-01	-4.89E-02	-4.61E-02
H8	9.54E-01	4.09E-01	3.47E-03	4.66E-02	1.02E-04	2.45E-04	1.18E-01	7.38E-01	-5.10E-02	-4.80E-02
Sum	3.20E+01	2.46E+01	1.58E+00	2.11E+01	2.96E-01	7.07E-01	1.46E+00	9.18E+00	3.64E-01	3.43E-01

Table 2 Acetic acid properties (see Fig. 1). The QTAIM number of electrons (population), localization index (LI), the second four largest eigenvalues, λ_i, listed in decreasing order, listed with the corresponding eigenvectors, and localization modes. Each mode is labelled whether it is a localization mode (the absolute value of at least one element of $\boldsymbol{v}_k$ is greater than or equal to 2) or delocalization mode (otherwise) where significant elements are shown in yellow and black respectively

Atom	Population	LI	ξ_5	v_5	ξ_6	v_6	ξ_7	v_7	ξ_8	v_8
			λ_5=0.3930 Delocalized		λ_6=0.3925 Delocalized		λ_7=0.2599 Delocalized		λ_8=6.0720E-02 Delocalized	
C1	4.43E+00	2.82E+00	-1.28E-03	-5.72E-06	-4.86E-06	-6.69E-11	2.72E-02	1.06E-02	4.38E-03	2.57E-04
O2	9.18E+00	8.29E+00	4.74E-05	2.11E-07	2.09E-07	2.87E-12	-2.60E-03	-1.01E-03	-7.32E-04	-4.30E-05
O3	9.12E+00	8.16E+00	4.78E-05	2.13E-07	2.81E-07	3.86E-12	-1.33E-03	-5.16E-04	-3.93E-02	-2.30E-03
H4	4.10E-01	7.32E-02	-1.61E-03	-7.18E-06	-3.44E-06	-4.73E-11	-3.10E-03	-1.20E-03	9.99E-01	5.86E-02
C5	5.98E+00	3.98E+00	-1.17E-03	-5.23E-06	-1.57E-06	-2.16E-11	-2.19E-01	-8.49E-02	-1.68E-03	-9.85E-05
H6	9.57E-01	4.10E-01	4.12E-01	1.84E-03	7.08E-01	9.74E-06	5.59E-01	2.17E-01	2.17E-03	1.27E-04
H7	9.57E-01	4.10E-01	4.15E-01	1.85E-03	-7.06E-01	-9.71E-06	5.59E-01	2.17E-01	2.17E-03	1.27E-04
H8	9.54E-01	4.09E-01	-8.11E-01	-3.62E-03	-1.76E-03	-2.42E-08	5.70E-01	2.21E-01	2.22E-04	1.30E-05
Sum	3.20E+01	2.46E+01	1.13E-02	5.05E-05	3.50E-05	4.82E-10	1.49E+00	5.77E-01	9.66E-01	5.67E-02

Table 3 Acetic acid properties (see Fig. 1). The QTAIM number of electrons (population), localization index (LI), and the sum of the localization modes

Atom	Population	LI	$v_1+v_3+v_8$
			Localized Sum
C1	4.43E+00	2.82E+00	3.53E+00
O2	9.18E+00	8.29E+00	1.06E+01
O3	9.12E+00	8.16E+00	7.22E+00
H4	4.10E-01	7.32E-02	3.42E-01
C5	5.98E+00	3.98E+00	6.31E+00
H6	9.57E-01	4.10E-01	7.84E-01
H7	9.57E-01	4.10E-01	7.84E-01
H8	9.54E-01	4.09E-01	7.85E-01
Sum	3.20E+01	2.46E+01	3.04E+01

transferring −1.34 electrons to O3. The net gain in O3 is 1.97 electrons.

Table 2 shows 4 weak modes where the electrons between the hydrogens are being transferred between them. Since the eigenvalues are small it is not expected to see a resonance structure, but rather an average between them. The mode with the smallest eigenvalue is associated with the hydrogen of the carboxylic acid. This hydrogen has the smallest number of localized electrons of any of the atoms and 80% of its localized electrons are contained within this mode, which may provide information regarding the transfer of this hydrogen in an acid-base reaction.

Table 3 shows that most of the electrons of the system are associated with 3 other modes. Approximately 2 electrons are associated with all the remaining delocalization modes.

4-bromonitrobenzene

Briefly, a summary of what the tables show. Tables 4 and 5 are associated with 4-Bromonitrobenzene with the atoms listed as in Fig. 2. The all contain the corresponding population (number of electrons) and LI for each atom for convenience.

- Table 4: associated with λ_1, λ_2, and λ_4 are localization modes, and associated with λ_3 is a delocalization mode.
- Table 5: associated with λ_5, λ_6, λ_7, and λ_8 are all delocalization modes.

Table 4 4-Bromonitrobenzene properties (see Fig. 2). The QTAIM population, localization index (LI), the first four largest eigenvalues, λ_i, listed in decreasing order, listed with the corresponding eigenvectors, and localization modes. Each mode is labelled if it is a localization mode (the absolute value of at least one element of $\boldsymbol{v}_k$ is greater than or equal to 2) or delocalization mode (otherwise) where significant elements are shown in yellow and black respectively

Atom	Population	LI	ξ_1	v_1	ξ_2	v_2	ξ_3	v_3	ξ_4	v_4
			λ_1=34.3310 Localized		λ_2=7.9350 Localized		λ_3=7.1207 Delocalized		λ_4=5.4347 Localized	
C1	5.97E+00	3.92E+00	3.88E-04	1.37E-02	1.88E-02	2.64E-01	-3.19E-03	-4.01E-08	4.02E-01	5.60E+00
C2	5.96E+00	3.91E+00	2.04E-03	7.17E-02	5.93E-03	8.35E-02	-5.64E-04	-7.08E-09	4.14E-01	5.77E+00
C3	6.09E+00	3.97E+00	1.89E-02	6.67E-01	4.56E-03	6.41E-02	-2.66E-07	-3.34E-12	4.15E-01	5.79E+00
C4	5.96E+00	3.91E+00	2.04E-03	7.17E-02	5.93E-03	8.35E-02	5.63E-04	7.07E-09	4.14E-01	5.77E+00
C5	5.97E+00	3.92E+00	3.88E-04	1.37E-02	1.88E-02	2.64E-01	3.19E-03	4.00E-08	4.02E-01	5.60E+00
C6	5.79E+00	3.77E+00	2.99E-04	1.05E-02	5.27E-02	7.41E-01	-2.21E-06	-2.77E-11	3.74E-01	5.21E+00
H7	9.04E-01	3.63E-01	4.16E-05	1.46E-03	3.15E-03	4.43E-02	-1.98E-03	-2.48E-08	4.05E-02	5.65E-01
H8	9.39E-01	3.95E-01	3.94E-04	1.39E-02	5.45E-04	7.67E-03	-2.20E-05	-2.77E-10	4.33E-02	6.03E-01
H9	9.39E-01	3.95E-01	3.94E-04	1.39E-02	5.45E-04	7.67E-03	2.20E-05	2.76E-10	4.33E-02	6.03E-01
H10	9.04E-01	3.63E-01	4.16E-05	1.46E-03	3.15E-03	4.43E-02	1.98E-03	2.48E-08	4.05E-02	5.65E-01
Br11	3.50E+01	3.43E+01	1.00E+00	3.52E+01	-2.11E-04	-2.96E-03	9.27E-09	1.16E-13	-1.00E-02	-1.40E-01
N12	6.59E+00	4.42E+00	4.65E-05	1.63E-03	3.23E-01	4.54E+00	-7.88E-06	-9.89E-11	9.47E-02	1.32E+00
O13	8.47E+00	7.32E+00	4.05E-05	1.43E-03	6.68E-01	9.39E+00	7.07E-01	8.87E-06	-5.42E-02	-7.56E-01
O14	8.47E+00	7.32E+00	4.05E-05	1.43E-03	6.68E-01	9.39E+00	-7.07E-01	-8.87E-06	-5.43E-02	-7.56E-01
Sum	9.80E+01	7.83E+01	1.02E+00	3.61E+01	1.77E+00	2.49E+01	1.76E-06	2.21E-11	2.56E+00	3.57E+01

The first localization mode can be associated with the bromine atom, see Table 4. The second localization mode can be associated with the nitro group, and the third localization mode (the fourth mode) is associated with the benzene group. The first delocalization mode (third mode) has a sum of nearly zero. This means both $\boldsymbol{\xi}_3$ and - $\boldsymbol{\xi}_3$ are valid. This can be associated with the resonance structures in the nitro group, that is, transferring electrons from O13 to O14 and also from O14 to O13. Table 5 shows several delocalization modes. These mainly show the redistribution of electrons within the benzene ring and the nitrogen receiving electrons from the oxygens.

10-hydroxy-10,9-borazarophenanthrene

Briefly, a summary of what the tables show. Tables 6 and 7 are associated with 10-hydroxy-10,9-borazarophenanthrene with the atoms listed as in Fig. 3. The all contain the corresponding population (number of electrons) and LI for each atom for convenience.

Table 5 4-Bromonitrobenzene properties (see Fig. 2). The QTAIM population, localization index (LI), the second four largest eigenvalues, λ_i, listed in decreasing order, listed with the corresponding eigenvectors, and localization modes. Each mode is labelled if it is a localization mode (the absolute value of at least one element of $\boldsymbol{v}_k$ is greater than or equal to 2) or delocalization mode (otherwise) where significant elements are shown in yellow and black respectively

Atom	Population	LI	ξ_5	v_5	ξ_6	v_6	ξ_7	v_7	ξ_8	v_8
			λ_5=4.5922		λ_6=4.5689		λ_7=3.9885		λ_8=3.3076	
C1	5.97E+00	3.92E+00	-4.98E-01	-1.39E-04	2.52E-01	1.13E-01	-2.67E-01	-1.30E-01	4.93E-01	2.05E-05
C2	5.96E+00	3.91E+00	-4.95E-01	-1.39E-04	-2.72E-01	-1.22E-01	2.18E-02	1.06E-02	-4.95E-01	-2.06E-05
C3	6.09E+00	3.97E+00	2.84E-04	7.96E-08	-5.35E-01	-2.40E-01	2.91E-01	1.42E-01	-1.11E-04	-4.59E-09
C4	5.96E+00	3.91E+00	4.95E-01	1.39E-04	-2.72E-01	-1.22E-01	2.18E-02	1.06E-02	4.96E-01	2.06E-05
C5	5.97E+00	3.92E+00	4.98E-01	1.39E-04	2.52E-01	1.13E-01	-2.67E-01	-1.30E-01	-4.93E-01	-2.05E-05
C6	5.79E+00	3.77E+00	-2.57E-04	-7.19E-08	5.36E-01	2.40E-01	-5.79E-02	-2.82E-02	-1.43E-04	-5.93E-09
H7	9.04E-01	3.63E-01	-5.62E-02	-1.57E-05	2.83E-02	1.27E-02	-3.45E-02	-1.68E-02	7.37E-02	3.06E-06
H8	9.39E-01	3.95E-01	-5.76E-02	-1.61E-05	-3.19E-02	-1.43E-02	2.96E-03	1.44E-03	-7.62E-02	-3.16E-06
H9	9.39E-01	3.95E-01	5.77E-02	1.61E-05	-3.18E-02	-1.43E-02	2.96E-03	1.44E-03	7.63E-02	3.16E-06
H10	9.04E-01	3.63E-01	5.62E-02	1.57E-05	2.84E-02	1.27E-02	-3.45E-02	-1.68E-02	-7.37E-02	-3.06E-06
Br11	3.50E+01	3.43E+01	-6.00E-06	-1.68E-09	1.09E-02	4.89E-03	-5.40E-03	-2.63E-03	1.71E-06	7.09E-11
N12	6.59E+00	4.42E+00	-1.71E-04	-4.79E-08	3.52E-01	1.58E-01	8.32E-01	4.05E-01	6.39E-05	2.65E-09
O13	8.47E+00	7.32E+00	-2.75E-03	-7.69E-07	-1.09E-01	-4.90E-02	-1.92E-01	-9.38E-02	2.02E-03	8.39E-08
O14	8.47E+00	7.32E+00	2.86E-03	8.00E-07	-1.09E-01	-4.90E-02	-1.92E-01	-9.38E-02	-2.05E-03	-8.49E-08
Sum	9.80E+01	7.83E+01	6.10E-05	1.71E-08	9.81E-02	4.40E-02	1.22E-01	5.95E-02	1.25E-05	5.20E-10

Table 6 10-hydroxy-10,9-borazarophenanthrene properties (see Fig. 3) The QTAIM population, localization index (LI), the first four largest eigenvalues, λ_i, listed in decreasing order, listed with the corresponding eigenvectors, and localization modes. Each mode is labelled if it is a localization mode (the absolute value of at least one element of $\boldsymbol{v}_k$ is greater than or equal to 2) or delocalization mode (otherwise) where significant elements are shown in yellow and black respectively

Atom	Population	LI	ξ_1	v_1	ξ_2	v_2	ξ_3	v_3	ξ_4	v_4
			$\lambda_1 = 8.5769$ Localized		$\lambda_2 = 7.0780$ Localized		$\lambda_3 = 5.7071$ Localized		$\lambda_4 = 5.3847$ Localized	
C1	6.02E+00	3.96E+00	2.00E-03	2.10E-02	7.39E-03	7.72E-02	3.01E-01	5.24E+00	-1.61E-01	-1.32E+00
C2	6.02E+00	3.95E+00	7.47E-03	7.85E-02	1.64E-02	1.72E-01	3.71E-01	6.46E+00	-1.81E-01	-1.48E+00
C3	6.65E+00	4.66E+00	2.59E-02	2.73E-01	5.40E-02	5.64E-01	5.49E-01	9.56E+00	-1.87E-01	-1.53E+00
C4	6.02E+00	3.90E+00	6.10E-03	6.41E-02	2.98E-02	3.12E-01	4.11E-01	7.16E+00	-4.83E-03	-3.95E-02
C5	6.02E+00	3.96E+00	1.68E-03	1.77E-02	1.04E-02	1.09E-01	3.13E-01	5.45E+00	-7.06E-02	-5.78E-01
C6	6.01E+00	3.95E+00	1.36E-03	1.43E-02	6.52E-03	6.81E-02	2.85E-01	4.95E+00	-1.26E-01	-1.03E+00
C7	6.00E+00	3.90E+00	3.84E-03	4.03E-02	5.92E-02	6.18E-01	2.25E-01	3.91E+00	3.09E-01	2.53E+00
C8	5.61E+00	3.59E+00	1.04E-02	1.09E-01	1.66E-01	1.74E+00	8.39E-02	1.46E+00	2.44E-01	2.00E+00
C9	6.02E+00	3.96E+00	3.14E-03	3.30E-02	5.85E-02	6.11E-01	7.91E-02	1.38E+00	3.76E-01	3.08E+00
H10	9.96E-01	4.39E-01	3.23E-04	3.40E-03	6.25E-03	6.53E-02	8.26E-03	1.44E-01	4.05E-02	3.32E-01
C11	6.01E+00	3.95E+00	1.02E-03	1.07E-02	2.29E-02	2.39E-01	8.95E-02	1.56E+00	4.43E-01	3.62E+00
C12	6.01E+00	3.96E+00	9.35E-04	9.83E-03	1.69E-02	1.77E-01	1.09E-01	1.89E+00	4.55E-01	3.72E+00
C13	6.01E+00	3.94E+00	1.11E-03	1.17E-02	2.20E-02	2.30E-01	1.50E-01	2.61E+00	4.09E-01	3.35E+00
H14	9.82E-01	4.32E-01	1.78E-04	1.87E-03	7.24E-04	7.56E-03	3.16E-02	5.50E-01	-1.74E-02	-1.43E-01
H15	9.61E-01	4.11E-01	1.92E-03	2.02E-02	1.34E-03	1.40E-02	3.77E-02	6.57E-01	-1.90E-02	-1.56E-01
H16	9.91E-01	4.27E-01	1.66E-04	1.74E-03	1.00E-03	1.04E-02	3.24E-02	5.65E-01	-6.68E-03	-5.46E-02
H17	9.82E-01	4.32E-01	1.24E-04	1.30E-03	6.22E-04	6.50E-03	2.98E-02	5.19E-01	-1.36E-02	-1.11E-01
H18	6.38E-01	1.77E-01	4.55E-03	4.79E-02	6.00E-02	6.27E-01	-6.69E-03	-1.16E-01	-6.53E-03	-5.34E-02
H19	9.79E-01	4.29E-01	9.63E-05	1.01E-03	2.21E-03	2.31E-02	9.37E-03	1.63E-01	4.78E-02	3.91E-01
H20	9.83E-01	4.31E-01	8.56E-05	9.00E-04	1.64E-03	1.71E-02	1.14E-02	1.99E-01	4.93E-02	4.03E-01
H21	9.85E-01	4.23E-01	1.02E-04	1.07E-03	2.12E-03	2.22E-02	1.59E-02	2.78E-01	4.31E-02	3.53E-01
N22	8.49E+00	6.95E+00	8.07E-02	8.48E-01	9.73E-01	1.02E+01	-9.98E-02	-1.74E+00	-9.27E-02	-7.59E-01
B23	2.83E+00	2.08E+00	3.83E-02	4.03E-01	4.50E-02	4.70E-01	3.23E-02	5.63E-01	-1.92E-02	-1.57E-01
O24	9.35E+00	8.54E+00	9.95E-01	1.05E+01	-8.48E-02	-8.86E-01	-1.67E-02	-2.90E-01	8.91E-03	7.29E-02
H25	4.34E-01	8.13E-02	3.99E-02	4.19E-01	-3.62E-03	-3.79E-02	-5.66E-04	-9.86E-03	3.56E-04	2.91E-03
Sum	1.02E+02	6.89E+01	1.23E+00	1.29E+01	1.48E+00	1.54E+01	3.05E+00	5.31E+01	1.52E+00	1.24E+01

- Table 6: associated with λ_1, λ_2, λ_3, and λ_4 are localization modes.
- Table 7: associated with λ_5, λ_6, λ_7, and λ_8 are all delocalization modes.

The first localization mode is associated with the hydroxyl group, O24 and H25, see Table 6. The second localization mode is associated with the nitrogen atom and its bonded hydrogen, N22 and H18. The third localization mode is associated with the benzene group, C1 to C6 with associated with hydrogens with a small role for C13. The fourth localization mode is associated with the benzene molecule, C7 to C9 and C11 to C13 with some association with the associated hydrogens. The next modes 4 modes, see Table 7, are delocalization modes that transfers electrons between the different rings. The boron atom, B23, contributes significantly to one of the weaker localization modes, the largest being with mode 15 (not shown) with an eigenvalue of 2.0318 that contributes a value in $\boldsymbol{v}_{15}$ of 1.74 electrons suggesting that boron's behaviour is more indirect in this chemical system.

Conclusion

The eigenvectors of the LDM and their associated localization and delocalization modes are introduced. The localization modes have been shown to determine the functional groups within a molecule. The delocalization modes have been shown to have modes that reflect resonance structures. As a result, the LDM and the associated eigenvalues, localization modes, and delocalization modes may be a powerful tool in determining resonance structures that reflect those used in organic chemistry and may be a useful tool in predicting reactivity where resonance has been used [1–5]. The larger eigenvalues associated with delocalization modes could be useful in determining where charge will accumulate. The modes associated with smaller eigenvalues may be useful in determining where electron flow is freer and may be subject to nucleophilic or electrophilic attack. The eigenvalues and eigenvectors can be interpreted similarly to those of the hardness matrix, or, more precisely, the negative inverse of the hardness matrix. This provides the energetic argument for associating the larger the eigenvalue the

Table 7 10-hydroxy-10,9-borazarophenanthrene properties (see Fig. 3). The QTAIM population, localization index (LI), the second four largest eigenvalues, λ_i, listed in decreasing order, listed with the corresponding eigenvectors, and localization modes. Each mode is labelled if it is a localization mode (the absolute value of at least one element of $\boldsymbol{v}_k$ is greater than or equal to 2) or delocalization mode (otherwise) where significant elements are shown in yellow and black respectively

Atom	Population	LI	ξ_5	v_5	ξ_6	v_6	ξ_5	v_5	ξ_6	v_6
			λ_5=4.8552 Delocalized		λ_6=4.7469 Delocalized		λ_7=4.5309 Delocalized		λ_8=4.3463 Delocalized	
C1	6.02E+00	3.96E+00	4.07E-01	1.65E+00	2.89E-01	4.34E-01	-2.36E-01	1.38E-02	3.10E-01	1.44E-01
C2	6.02E+00	3.95E+00	-5.50E-02	-2.23E-01	4.05E-01	6.08E-01	-2.03E-01	1.18E-02	2.24E-01	1.05E-01
C3	6.65E+00	4.66E+00	-5.43E-01	-2.20E+00	1.87E-01	2.81E-01	6.65E-02	-3.88E-03	-1.83E-01	-8.53E-02
C4	6.02E+00	3.90E+00	-1.70E-01	-6.91E-01	-3.64E-01	-5.47E-01	2.05E-01	-1.19E-02	-1.45E-01	-6.74E-02
C5	6.02E+00	3.96E+00	3.49E-01	1.41E+00	-3.71E-01	-5.58E-01	2.27E-01	-1.32E-02	-3.15E-01	-1.47E-01
C6	6.01E+00	3.95E+00	5.82E-01	2.36E+00	-8.30E-02	-1.25E-01	8.58E-03	-5.00E-04	-5.59E-02	-2.60E-02
C7	6.00E+00	3.90E+00	-1.14E-01	-4.60E-01	-3.93E-01	-5.90E-01	-7.86E-02	4.58E-03	4.50E-01	2.10E-01
C8	5.61E+00	3.59E+00	-3.53E-03	-1.43E-02	-5.06E-02	-7.59E-02	2.55E-01	-1.49E-02	4.37E-01	2.03E-01
C9	6.02E+00	3.96E+00	8.52E-02	3.45E-01	2.89E-01	4.33E-01	5.26E-01	-3.07E-02	1.82E-01	8.46E-02
H10	9.96E-01	4.39E-01	9.78E-03	3.96E-02	3.35E-02	5.04E-02	6.34E-02	-3.70E-03	2.27E-02	1.06E-02
C11	6.01E+00	3.95E+00	1.07E-01	4.33E-01	3.65E-01	5.48E-01	2.07E-01	-1.21E-02	-3.07E-01	-1.43E-01
C12	6.01E+00	3.96E+00	5.39E-02	2.18E-01	1.34E-01	2.01E-01	-3.74E-01	2.18E-02	-3.95E-01	-1.84E-01
C13	6.01E+00	3.94E+00	-3.55E-02	-1.44E-01	-2.00E-01	-3.00E-01	-5.07E-01	2.96E-02	5.62E-02	2.62E-02
H14	9.82E-01	4.32E-01	4.69E-02	1.90E-01	3.38E-02	5.08E-02	-2.85E-02	1.66E-03	3.86E-02	1.80E-02
H15	9.61E-01	4.11E-01	-5.86E-03	-2.37E-02	4.61E-02	6.92E-02	-2.40E-02	1.40E-03	2.75E-02	1.28E-02
H16	9.91E-01	4.27E-01	3.94E-02	1.59E-01	-4.29E-02	-6.44E-02	2.57E-02	-1.50E-03	-3.85E-02	-1.79E-02
H17	9.82E-01	4.32E-01	6.70E-02	2.72E-01	-9.78E-03	-1.47E-02	1.09E-03	-6.33E-05	-6.98E-03	-3.25E-03
H18	6.38E-01	1.77E-01	2.01E-03	8.16E-03	4.54E-04	6.82E-04	-5.11E-03	2.98E-04	-7.25E-03	-3.37E-03
H19	9.79E-01	4.29E-01	1.23E-02	4.98E-02	4.26E-02	6.40E-02	2.51E-02	-1.46E-03	-3.81E-02	-1.77E-02
H20	9.83E-01	4.31E-01	6.19E-03	2.51E-02	1.56E-02	2.35E-02	-4.53E-02	2.64E-03	-4.93E-02	-2.29E-02
H21	9.85E-01	4.23E-01	-3.10E-03	-1.26E-02	-2.37E-02	-3.56E-02	-5.93E-02	3.46E-03	6.05E-03	2.82E-03
N22	8.49E+00	6.95E+00	2.81E-02	1.14E-01	3.45E-03	5.18E-03	-6.45E-02	3.76E-03	-8.58E-02	-4.00E-02
B23	2.83E+00	2.08E+00	-4.43E-02	-1.79E-01	1.67E-02	2.51E-02	1.25E-03	-7.26E-05	-2.61E-02	-1.22E-02
O24	9.35E+00	8.54E+00	1.29E-02	5.21E-02	-5.68E-03	-8.53E-03	5.38E-04	-3.13E-05	5.65E-03	2.63E-03
H25	4.34E-01	8.13E-02	4.27E-04	1.73E-03	-2.49E-04	-3.74E-04	7.30E-05	-4.25E-06	2.08E-04	9.70E-05
Sum	1.02E+02	6.89E+01	8.35E-01	3.38E+00	3.16E-01	4.75E-01	-1.29E-02	7.50E-04	1.07E-01	4.99E-02

greater the energetic resistance to the transfer within a pattern as prescribed by the eigenvector.

Appendix A: Hardness Matrix Interpretation

The first part of this appendix will provide an interpretation of the eigenvalues and eigenvectors of the hardness matrix to energetic stability of a pattern. The second part will be relating the LDM to the hardness matrix and justifying interpreting the eigenvectors of the hardness matrix as those of the LDM.

Consider the energy as a function of the electron population of each atom, N, expanded as a Taylor series about the original number of electrons for each atom, N_0, truncated at second order

$$E(N) = E(N_0) + \mu\,\uparrow^T (N - N_0) + \frac{1}{2}(N - N_0)^T \eta (N - N_0) \tag{15}$$

where $(N - N_0)^T$ is the transpose of $N - N_0$,

$$\left.\frac{\partial EN}{\partial N_i}\right|_{N=N_0} = \mu \tag{16}$$

due to electronegativity equalization, and the elements of the hardness matrix, η, are

$$\eta_{ij} = \frac{\partial E(N(\Omega_1), \ldots, N(\Omega_n))}{\partial N(\Omega_i)\partial N(\Omega_j)} \tag{17}$$

Next consider adding a perturbation $V(N)$ expanded by a Taylor series about the original number of electrons for each atom, N_0 truncated at first order is

$$V(N) = V(N_0) + \chi^T (N - N_0) \tag{18}$$

where the i^{th} element of χ, χ_i, is

$$\left.\frac{\partial VN}{\partial N_i}\right|_{N=N_0} = \chi_i \tag{19}$$

The new total energy within this framework

$$E(N)+V(N)=E(N_0)+\mu 1^T(N-N_0)+\frac{1}{2}(N-N_0)^T\eta(N-N_0)+V(N_0)+\chi^T(N-N_0) \quad (20)$$

Next find the N that minimizes the energy, N_{min}, that yields the lowest energy

$$\frac{\partial(E(N)+V(N))}{\partial N}=\mu 1+\eta(N-N_0)+\chi=0 \quad (21)$$

yielding the N_{min} of

$$N_{min}=N_0-\eta^{-1}(\chi-\mu 1) \quad (22)$$

To find the energy insert N_{min} into the energy expression in Eq. (23)

$$E(N_{min})+V(N_{min})=E(N_0)-\frac{1}{2}((\chi-\mu 1))^T\eta^{-1}((\chi-\mu 1))+V(N_0) \quad (23)$$

Next expand the vector that minimizes the energy, Eq. (24), in terms of an orthonormal set of eigenvectors of η denoted η_i.

$$\chi-\mu 1=\sum_{i=1}^{n}c_i\eta_i \quad (24)$$

where the c_i's are exactly

$$c_i=(\chi-\mu 1)^T\eta_i \quad (25)$$

Provided that η^{-1} exists then the eigenvectors of η^{-1} are the same as η. Taking the eigenvector η_i of η has eigenvalue η_i the eigenvector η_i of η^{-1} has eigenvalue $1/\eta_i$. Thus,

$$\left(\sum_{i=1}^{n}\frac{c_i}{\eta_i}\eta_i\right)\eta^{-1}\sum_{i=1}^{n}c_i\eta_i=\sum_{i=1}^{n}\frac{c_i^2}{\eta_i} \quad (26)$$

This means the smallest positive eigenvalues of the hardness matrix generally lead to larger coefficients. Therefore the eigenvectors with the smallest positive eigenvalues will generally be the modes activated. Given the argument here that the hardness matrix is related to the LDM this analogy suggest that a small perturbation will generally cause electrons to flow in the eigenvectors associated with small eigenvalues as expected. Furthermore this means that the negative eigenvalues will increase the energy, suggesting avoidance of the modes associated with negative eigenvalue especially those small in magnitude, which is generally the case by the restriction that the sum of the diagonal elements of a matrix is the sum of the eigenvalues, Eq. (12).

The next step is to relate the hardness matrix to the inverse of the covariance matrix and from there to relate it to the LDM. Start from the grand canonical partition function

$$Z(\mu_1,\ldots,\mu_n)=\text{Tr}\left(e^{-\beta\left(\hat{H}_0-\sum_{k=1}^{n}\mu_k\hat{N}_k\right)}\right) \quad (27)$$

where β is the thermodynamic β, the Hamiltonian, μ_k is the chemical potential of atom k, $\hat{N}_k$ the population operator of atom k, and Tr is the trace operator. We define explicitly the expectation value of $\hat{N}_k$ as is

$$\langle\hat{N}_k\rangle=N(\Omega_k)=N_k \quad (28)$$

and

$$\langle\hat{N}_j\hat{N}_k\rangle-\langle\hat{N}_j\rangle\langle\hat{N}_k\rangle=-\frac{\delta(\Omega_j,\Omega_k)}{2}j\neq k \quad (29)$$

However,

$$\langle\hat{N}_i\hat{N}_i\rangle-\langle\hat{N}_i\rangle^2=-\Lambda(\Omega_i)+N(\Omega_i) \quad (30)$$

This leads to the covariance matrix, Æ, where the k^{th} diagonal element is Eq. (30) and the j,k^{th} off-diagonal elements are given by Eq. (29) leading to

$$Æ=-\zeta+\Omega \quad (31)$$

where the k^{th} diagonal element of the diagonal matrix Ω is $N(\Omega_k)$. If the Ω matrix is neglected then the covariance matrix as introduced by Ayers will be yielded. [120]

The next steps investigate the derivatives of the free energy and a Legendre transform of the free energy showing that the covariance matrix is proportional to the inverse of the hardness matrix. The covariance matrix will be related to the LDM as the negative of the LDM through this derivation. Defining the free energy as

$$F(\mu_1,\ldots,\mu_n)=-\frac{1}{\beta}1n\ Z(\mu_1,\ldots,\mu_n) \quad (32)$$

and differentiate with respect to the free energy with respect to μ_i and μ_j yields

$$\begin{aligned}\frac{\partial^2F(\mu_1,\ldots,\mu_n)}{\partial\mu_j\partial\mu_i}&=\frac{\partial N(\Omega_i)}{\partial\mu_j}\\&=-\frac{1}{Z(\mu_1,\ldots,\mu_n)}\text{Tr}\left(\beta\hat{N}_je^{-\beta\left(\hat{H}_0-\sum_{k=1}^{n}\mu_k\hat{N}\right)}\right)+\frac{1}{(Z(\mu_1,\ldots,\mu_n))}\text{Tr}\left(\hat{N}_ie^{-\beta\left(\hat{H}_0-\sum_{k=1}^{n}\mu_k\hat{N}\right)}\right)\text{Tr}\left(\beta\hat{N}_je^{-\beta\left(\hat{H}_0-\sum_{k=1}^{n}\mu_k\hat{N}\right)}\right)\\&=-\beta(\langle\hat{N}_i\hat{N}_j\rangle-\langle\hat{N}_i\rangle\langle\hat{N}_j\rangle)\beta\zeta_{ij}+\beta\Omega\end{aligned} \quad (33)$$

which is the covariance matrix scaled by -β. Next consider the Legendre transform of the free energy

$$E(N(\Omega_1),\ldots,N(\Omega_N))=F(\mu_1,\ldots,\mu)+\sum_{k=1}^{n}\mu_kN(\Omega_k) \quad (34)$$

and then differentiating with respect to the new variables leads to $N(\Omega_i)$

$$\frac{\partial E(N(\Omega_1),\ldots,N(\Omega_N))}{\partial N(\Omega_i)} = \sum_{k=1}^{n}\left(\frac{\partial F(\mu_1,\ldots,\mu_n)}{\partial \mu_k}\frac{\partial \mu_k(\mu_1,\ldots,\mu_n)}{\partial N(\Omega_i)} + \frac{\partial \mu_k(\mu_1,\ldots,\mu_n)}{\partial N(\Omega_i)}N(\Omega_k)\right) + \mu_i \tag{35}$$

And using the result from Eq. (33) we find

$$\frac{\partial E(N(\Omega_1),\ldots,N(\Omega_N))}{\partial N(\Omega_i)} = \sum_{k=1}^{n}\left(-N(\Omega_k)\frac{\partial \mu_k(\mu_1,\ldots,\mu_n)}{\partial N(\Omega_i)} + \frac{\partial \mu_k(u_1,\ldots,\mu_n)}{\partial N(\Omega_i)}N(\Omega_k)\right) + \mu_i = \mu_i \tag{36}$$

then differenting again with respect $N(\Omega_j)$ yields

$$\frac{\partial^2 E(N(\Omega_1),\ldots,n(\Omega_N))}{\partial N(\Omega_j)\partial N(\Omega_i)} = \frac{\partial \mu_i}{\partial N(\Omega_j)} = \eta_{ij} \tag{37}$$

which is just the i,j^{th} element of the hardness matrix. Taking the inverse of the hardness matrix and noting the relationships in Eqs. (31) and (33) yields the relationship between the hardness matrix and the covariance matrix

$$\eta^{-1} = \beta Æ = -\beta\zeta + \beta\Omega \tag{38}$$

The relationship between the inverse of a Hessian and the covariance matrix is known in other contexts as well [121–123]. If the matrix Ω is neglected then LDM is exactly proportional to the inverse of the hardness matrix. Furthermore, if Ω commutes with the LDM then they have the same eigenvectors as the inverse of the hardness matrix. An example where the LDM commutes with Ω is when the off-diagonal elements of the LDM matrix are zero. This would approximately be the case where the electrons in the chemical system are nearly all localized to the individual atoms. This would also happen in systems where all atoms are equivalent like the hydrogen dimer. We also know from the Davis-Kahan sine theorem [79] that an eigenvectors associated with an eigenvalue that is well spaced from other eigenvalues in an absolute difference sense will not rotate substantially. Noting that frequently in chemical systems many atoms will have the same or similar populations meaning that there are more than n eigenvectors for Ω. This suggests that even in cases where Ω does not commute with the LDM often many of the eigenvectors of the LDM will also be an eigenvector of Ω and thus an eigenvector of the hardness matrix. Taking the positive eigenvalues of the hardness matrix to be

$$\eta_1^+ \leq \eta_2^+ \leq \ldots \tag{39}$$

Then the corresponding eigenvalues of the negative if the inverse of the hardness matrix are

$$-\frac{1}{\eta_1^+} \leq -\frac{1}{\eta_2^+} \leq \ldots \tag{40}$$

where the order has been preserved. The order is preserved amongst negative eigenvalues as well. However, the negative eigenvalues of the hardness matrix are now positive and vice versa. And in the case where the population of each of the atoms are nearly equal the eigenvalues of the negative inverse of the hardness matrix are shifted by a constant thus preserving the order of the eigenvalues between theLDM and the negative inverse of the hardness matrix.

Appendix B: Mode Vector

Consider a vector $v_k$where the sum of all v_k will yield the population of atom *k* is found in the k^{th} element. Thus

$$\sum_k v_k = \zeta \,\text{⅂} \tag{41}$$

where ⅂ is a column vector where every element is one. Since the LDM is symmetric it can always bediagonalized. First expand the ⅂ vector in terms of the eigenvectors of the LDM

$$\text{⅂} = \sum_{i=1}^{n} c_i\xi_i \tag{42}$$

where c_i is a coefficient. Multiplying both sides by the vector ξ_i^T and recalling that eigenvectors of theLDM are real and orthonormal yields

$$\xi_i^T\,\text{⅂} = c_i \tag{43}$$

Thus the ⅂ vector can be written as

$$1 = \sum_{i=1}^{n}(\xi_i^T 1) = \sum_{i=1}^{n}\left(\sum_j \xi_{j,i}\right)\xi_i \tag{44}$$

Applying the LDM to the ⅂ vector yields

$$\zeta\,\text{⅂} = \sum_{i-1}^{n}\lambda_i\left(\sum_j \xi_{j,i}\right)\xi_i = \begin{bmatrix} N(\Omega_1) \\ N(\Omega_2) \\ \vdots \\ N(\Omega_n) \end{bmatrix} \tag{45}$$

Finally, v_i can be found by choosing each v_i to be the i^{th} term in the sum over i, thus

$$v_i = \lambda_i\left(\sum_j \xi_{j,i}\right)\xi_i \tag{46}$$

Notice that if ξ_i is replaced with $-\xi_i$

$$\lambda_i \left(\sum_j -\xi_{j,i} \right) (-\xi_i) = \lambda_i \left(\sum_j -\xi_{j,i} \right) (-\xi_i) = v_i \qquad (47)$$

thus v_i is unchanged regardless if ξ_i or $-\xi_i$ is chosen. Notice also that if $\sum_j \xi_{j,i} = 0$ or $\lambda_i = 0$ then v_i is the zero vector. This is why for these cases both ξ_i and $-\xi_i$ can be considered and both can be interpreted as resonance structures restoring to the other form.

Acknowledgements JSMA gratefully acknowledges the support of PAPIIT-DGAPA-UNAM IA203921, PAPIIT-DGAPA-UNAM IA210123, and PAPIIT-DGAPA-UNAM IN223725. JSMA thanks Compute Canada/Digital Research Alliance of Canada for granting access to computational resources. JSMA extends appreciation to DGTIC/UNAM for computer time in the project LANCAD-UNAM-DGTIC 378.

Author contributions JSMA is the sole author carried out all aspects of the research and all preparations of this article.

Funding JSMA gratefully acknowledges the support of PAPIIT-DGAPA-UNAM IA203921, PAPIIT-DGAPA-UNAM IA210123, and PAPIIT-DGAPA-UNAM IN223725. JSMA thanks Compute Canada/Digital Research Alliance of Canada for granting access to computational resources. JSMA extends appreciation to DGTIC/UNAM for computer time in the project LANCAD-UNAM-DGTIC 378.

Data availability All data is available upon request.

Declarations

Ethics Not applicable.

Competing interests The authors declare no competing interests.

References

1. Carey FA, Sundberg RJ (1984) Advanced Organic Chemistry, Part A: Structure and Mechanism. Plenum, New York
2. Kekulé A (1865) Sur la constitution des substances aromatiques. Bull Soc Chim Paris N S 3:98
3. Kekulé A (1865) Note sur quelques produits de substitution de la benzine. Bull Acad R Belg 19:551–563
4. Kekuié A (1866) Untersuchungen über aromatische Verbindungen Ueber die Constitution der aromatischen Verbindungen. I. Ueber die Constitution der aromatischen Verbindungen. Liebigs Ann 137:129–196
5. Dewar J (1869) 5. On the Oxidation of Phenyl Alcohol, and a Mechanical Arrangement adapted to illustrate Structure in the Nonsaturated Hydrocarbons. Proc. Roy. Soc. Edinburgh 6:82–86
6. Levine IN (2014) Quantum chemistry. Pearson, Boston
7. Bader RFW (1990) Atoms in Molecules: A Quantum Theory. Clarendon, Oxford
8. Matta CF, Boyd RJ (2007) In:C. F. Matta and R. J. Boyd (eds) Quantum theory of atoms in molecules: recent progress in theory and application, Wiley-VCH, Weinheim
9. Cortés-Guzmán F, Rodríguez JI, Anderson JSM (2023) In:J. I. Rodríguez, F. Cortés-Guzmán and J. S. M. Anderson (eds) Advances in Quantum Chemical Topology Beyond QTAIM, Elsevier, Amsterdam, Netherlands
10. Popelier PLA (2000) Atoms in Molecules: An Introduction. Pearson, Harlow
11. Rodríguez JI, Cortés-Guzmán F, Anderson JSM (2023) Advances in quantum chemical topology beyond QTAIM. Elsevier, Amsterdam, Netherlands
12. Bader RFW, Stephens ME (1974) Fluctuation and correlation of electrons in molecular systems. Chem Phys Lett 26:445–449
13. Bader RFW, Stephens ME (1975) Spatial localization of the electronic pair and number distributions in molecules. J Am Chem Soc 97:7391–7399
14. Outeiral C, Vincent MA, Martín Pendás Á, Popelier PLA (2018) Revitalizing the concept of bond order through delocalization measures in real space. Chem Sci 9:5517–5529
15. Matta CF (2014) Modeling biophysical and biological properties from the characteristics of the molecular electron density, electron localization and delocalization matrices, and the electrostatic potential. J Comput Chem 35:1165–1198
16. Matta CF, Ayers PW, Cook R (2024) Electron Localization-Delocalization Matrices. Springer International Publishing, Cham
17. Cortés-Guzmán F, Bader RFW (2005) Complementarity of QTAIM and MO theory in the study of bonding in donor–acceptor complexes. Coord Chem Rev 249:633–662
18. Fradera X, Austen MA, Bader RFW (1999) The Lewis Model and Beyond. J Phys Chem A 103:304–314
19. Matta CF, Sumar I, Cook R, Ayers PW (2016) In: Chauvin R, Lepetit C, Silvi B, Alikhani E (eds) Applications of Topological Methods in Molecular Chemistry. Springer International Publishing, Cham
20. Timm MJ, Matta CF, Massa L, Huang L (2014) The localization–delocalization matrix and the electron-density-weighted connectivity matrix of a finite graphene nanoribbon reconstructed from kernel fragments. J Phys Chem A 118:11304–11316
21. Setiawan D, Kraka E, Cremer D (2016) Quantitative Assessment of Aromaticity and Antiaromaticity Utilizing Vibrational Spectroscopy. J Org Chem 81:9669–9686
22. Li T, Huls NJ, Lu S, Hou P (2024) Unsupervised manifold embedding to encode molecular quantum information for supervised learning of chemical data. Commun Chem 7:133
23. Al-Otaibi JS, Mary YS, Mondal A, Acharjee N, Gamberini MC (2025) Computational Insight into the Non-Covalent Binding of Amiloride with Sumanene: A DFT and QTAIM Perspective. ChemistrySelect 10:e03215
24. Saha P, Sharma M, Balaji S, Barsainyan AA, Kumar R, Steuber V, Schmuker M (2025) Dense Sense: a novel approach utilizing electron density augmented machine learning paradigm to understand the complex odour landscape. Digit Discov 4:3339–3350
25. Pilmé J, Spezia R (2023) Diabolus in Chemistry? ChemRxiv. Camebridge Open Engage, Camebridge

26. Woolever M, Nabity J, Cook R, Fox E (2023) Ionic Liquid Parameter Prediction Leveraging Quantum Structure Property Relationships. 52nd International Conference on Environmental Systems
27. Dittrich B, Matta CF (2014) Contributions of charge-density research to medicinal chemistry. IUCrJ 1:457–469
28. Terrabuio LA, Haiduke RLA, Matta CF (2016) Difluorodiazirine (CF2N2): A comparative quantum mechanical study of the first triplet and first singlet excited states. Chem Phys Lett 655–656:96–102
29. Matta CF, Hutter MC (2018) Ask the Experts: Computational Chemistry. Future Med Chem 10:1521–1524
30. Koch D, Pavanello M, Shao X, Ihara M, Ayers PW, Matta CF, Jenkins S, Manzhos S (2024) The Analysis of Electron Densities: From Basics to Emergent Applications. Chem Rev 124:12661–12737
31. Genoni A, Bučinský L, Claiser N, Contreras-García J, Dittrich B, Dominiak PM, Espinosa E, Gatti C, Giannozzi P, Gillet J-M, Jayatilaka D, Macchi P, Madsen AØ, Massa L, Matta CF, Merz Jr. (2018) In: Nakashima PNH, Ott H, Ryde U, Schwarz K, Sierka M, Grabowsky S (eds) Quantum Crystallography: Current Developments and Future Perspectives, vol 24. KM, pp 10881–10905
32. Sadjadi S, Matta CF, Hamilton IP (2021) Bonding and metastability for Group 12 dications. J Comput Chem 42:40–49
33. Castanedo LAM, Matta CF, Ylijoki KEO (2022) The reaction path of cyclooctatetraene dimerization revisited. Int J Quantum Chem 122:e26866
34. Massa L, Castanedo LAM, Fahimi P, Matta CF (2023) In: Thomas ME, Thomas J, Thomas S, Kornweitz H (eds) In silico Approaches to Macromolecular Chemistry. Elsevier, Amsterdam, Netherlands
35. Sumar I, Cook R, Ayers PW, Matta CF (2015) AIMLDM: A program to generate and analyze electron localization–delocalization matrices (LDMs). 1070:55–67
36. Keith TA (2019) AIMALL 19.10.12 aim.tkgristmill.com (19.10.12). AIMALL 19.10.12 aim.tkgristmill.com Gristmill Software, Overland Park, KS, USA
37. Sumar I, Cook R, Ayers PW, Matta CF (2016) Aromaticity of rings-in-molecules (RIMs) from electron localization–delocalization matrices (LDMs)*. 91:013001
38. Cook RL (2017) Principal components of localization-delocalization matrices: new descriptors for modeling biological activities of organic compounds. Part I: mosquito insecticides and repellents. 28:1525–1535
39. Sumar I, Ayers PW, Matta CF (2014) Electron localization-delocalization matrices in the prediction of pKa's and UV-wavelengths of maximum absorbance of p-benzoic acids and the definition of super-atoms in molecules. 612:190–197
40. Bader RFW, Nguyen-Dang TT (1981) Quantum-Theory of Atoms in Molecules -. Dalton Revisit 14:63–124
41. Zadeh FH, Shahbazian S (2011) Toward a fuzzy atom view within the context of the quantum theory of atoms in molecules: quasi-atoms. Theor Chem Acc 128:175–181
42. Heidarzadeh F, Shahbazian S (2011) The Quantum Divided Basins: A New Class of Quantum Subsystems. Int J Quantum Chem 111:2788–2801
43. Cioslowski J, Karwowski J (2001) In:R. Carbó-Dorca and X. Gironés (eds) Fundamentals of molecular similarity, Kluwer, Dordrecht
44. Anderson JSM (2023) In:J. I. Rodríguez, F. Cortés-Guzmán and J. S. M. Anderson (eds) Advances in Quantum Chemical Topology Beyond QTAIM, Elsevier, Amsterdam, Netherlands
45. Anderson JSM, Ayers PW (2011) Quantum Theory of Atoms in Molecules: Results for the SR-ZORA Hamiltonian. J Phys Chem A 115:13001–13006
46. Anderson JSM, Ayers PW (2018) The general setting for the zero-flux condition: The Lagrangian and zero-flux conditions that give the Heisenberg equation of motion. J Comp Chem 39:1051–1058
47. Zapata-Escobar AD, Maldonado AF (2025) Relativistic definitions of atoms in molecules with the modified Dirac equation. J Chem Phys 163
48. Cassam-Chenai P, Jayatilaka D (2001) Some fundamental problems with zero flux partitioning of electron densities. Theor Chem Acc 105:213–218
49. Bader RFW (2002) A comment on some fundamental problems with zero-flux partitioning of electron densities. Theor Chem Acc 107:381–382
50. Cassam-Chenai P, Jayatilaka D (2002) A complement to some fundamental problems with zero flux partitioning of electron densities. Theor Chem Acc 107:383–384
51. Cassam-Chenai P (2002) Frequently asked questions on Some fundamental problems with zero flux partitioning of electron densities. J Math Chem 31:145–153
52. Delle Site L (2002) Bader's interatomic surfaces are unique. Theor Chem Acc 107:378–380
53. Mohallem JR (2002) Molecular structure and Bader's theory. Theor Chem Acc 107:372–374
54. Anderson JSM, Ayers PW, Hernandez JIR (2010) How ambiguous is the local kinetic energy? J Phys Chem A 114:8884–8895
55. Cohen L (1984) Representable local kinetic energy. J CHem Phys 80:4277–4279
56. Cohen L (1979) Local kinetic energy in quantum mechanics. J Chem Phys 70:788–789
57. Morgenstern A (2023) In:J. I. Rodríguez, F. Cortés-Guzmán and J. S. M. Anderson (eds) Advances in Quantum Chemical Topology Beyond QTAIM, Elsevier, Amsterdam, Netherlands
58. Jones TE, Eberhart ME (2010) The bond bundle in open systems. Int J Quantum Chem 110:1500–1505
59. Eberhart M (2001) A quantum description of the chemical bond. Philos Mag B 81:721–729
60. Morgenstern A, Wilson TR, Eberhart ME (2017) Predicting Chemical Reactivity from the Charge Density through Gradient Bundle Analysis: Moving beyond Fukui Functions. J Phys Chem A 121:4341–4351
61. Morgenstern A, Morgenstern C, Miorelli J, Wilson T, Eberhart ME (2016) The influence of zero-flux surface motion on chemical reactivity. Phys Chem Chem Phys 18:5638–5646
62. Morgenstern A, Wilson T, Miorelli J, Jones T, Eberhart ME (2015) In search of an intrinsic chemical bond. Comput Theor Chem 1053:31–37
63. Anderson JSM, Mortera-Carbonell AJ, Matta CF (2023) In:J. I. Rodríguez, F. Cortés-Guzmán and J. S. M. Anderson (eds) Advances in Quantum Chemical Topology Beyond QTAIM, Elsevier, Amsterdam, Netherlands
64. Anderson JSM, Massa L, Matta CF (2021) Non-Nuclear maxima and the universality of Bright Wilson's justification of the first Hohenberg Kohn theorem revisited. Chem Phys Lett 780:138940
65. Pendás AM, Blanco MA, Francisco E (2007) Chemical fragments in real space: Definitions, properties, and energetic decompositions. J Comput Chem 28:161–184
66. Geerlings P, De Proft F, Langenaeker W (2003) Conceptual density functional theory. Chem Rev 103:1793–1873
67. Nalewajski RF, Korchowiec J, Zhou Z (1988) Molecular hardness and softness parameters and their use in chemistry. Int J Quantum Chem 22:349–366
68. Nalewajski RF (1994) Sensitivity analysis of charge transfer systems: in situ quantities, intersecting state model and its implications. Int J Quantum Chem 49:675–703
69. Komorowski L (1993) In: Sen KD (ed) Chemical Hardness. Springer, Berlin Heidelberg, Berlin, Heidelberg

70. Nalewajski RF (1993) The hardness-based, molecular-charge sensitivities and their use in the theory of chemical reactivity. Struct Bonding 80:115–186
71. Baekelandt BG, Mortier WJ, Schoonheydt RA (1993) In: Sen KD (ed) Chemical Hardness. Springer, Berlin Heidelberg, Berlin, Heidelberg
72. Nalewajski RF (1991) Normal (decoupled) representation of electronegativity equalization equations in a molecule. Int J Quantum Chem 40:265–285
73. Nalewajski RF, Korchowiec J (1990) Protonation of pyrrole: a model hardness (softness) sensitivity study. Croat Chem Acta 62:603–616
74. Nalewajski RF (1992) Internal orbitally resolved charge sensitivity analysis. Int J Quantum Chem 44:67–80
75. Neshev N, Mineva TZ (1996) In:N. Russo and D. R. Salahub (eds) Metal-Ligand Interactions: Structure and Reactivity, Springer Netherlands, Dordrecht
76. Cioslowski J, Martinov M (1994) The atomic softness matrix. J Chem Phys 101:366–370
77. Verstraelen T, Ayers PW, Van Speybroeck V, Waroquier M (2013) ACKS2: Atom-condensed Kohn-Sham DFT approximated to second order. J Chem Phys 138:074108
78. Weyl H (1912) Das asymptotische Verteilungsgesetz der Eigenwerte linearer partieller Differentialgleichungen (mit einer Anwendung auf die Theorie der Hohlraumstrahlung). 71:441–479
79. Davis C, Kahan WM (1970) The Rotation of Eigenvectors by a Perturbation. III. SIAM J Numer Anal 7:1–46
80. Kohn W, Sham LJ (1965) Self-consistent equations including exchange and correlation effects. Phys Rev 140:A1133–A1138
81. Hohenberg P, Kohn W (1964) Inhomogeneous electron gas. Phys Rev 136:B864–B871
82. Parr RG, Yang W (1989) Density-Functional Theory of Atoms and Molecules. Oxford UP, New York
83. Koch W, Holthausen MC (2001) A chemist's guide to density functional theory. Wiley-VCH, New York
84. Mardirossian N, Head-Gordon M (2014) ωB97X-V: A 10-parameter, range-separated hybrid, generalized gradient approximation density functional with nonlocal correlation, designed by a survival-of-the-fittest strategy. Phys Chem Chem Phys 16:9904–9924
85. Chai J-D, Head-Gordon M (2008) Systematic optimization of long-range corrected hybrid density functionals. J Chem Phys 128:084106
86. Becke AD (1997) Density-functional thermochemistry. V. Systematic optimization of exchange-correlation functionals. J Chem Phys 107:8554–8560
87. Krishnan R, Binkley JS, Seeger R, Pople JA (1980) Self-consistent molecular-orbital methods.20. Basis set for correlated wavefunctions. J Chem Phys 72:650–654
88. Clark T, Chandrasekhar J, Spitznagel GW, Schleyer PVR (1983) Efficient diffuse function-augmented basis sets for anion calculations. III. The 3–21+G basis set for first-row elements, Li–F. J Comput Chem 4:294–301
89. Curtiss LA, McGrath MP, Blaudeau JP, Davis NE, Binning RC Jr., Radom L (1995) Extension of Gaussian-2 theory to molecules containing third-row atoms Ga–Kr. J Chem Phys 103:6104–6113
90. Neese F (2025) Software Update: The ORCA Program System—Version 6.0. WIREs Comput Mol Sci 15:e70019
91. Neese F (2023) The SHARK integral generation and digestion system. J Comput Chem 44:381–396
92. Neese F (2012) The ORCA program system. Wiley Interdiscip Rev -Comput Mol Sci 2:73–78
93. Neese F (2018) Software update: the ORCA program system, version 4.0. WIREs Comput Mol Sci 8:e1327
94. Neese F, Wennmohs F, Becker U, Riplinger C (2020) The ORCA quantum chemistry program package. J Chem Phys 152:224108
95. Neese F (2022) Software update: The ORCA program system—Version 5.0. WIREs Comput Mol Sci 12:e1606
96. Neese F (2000) Approximate second-order SCF convergence for spin unrestricted wavefunctions. Chem Phys Lett 325:93–98
97. Chang C, Pelissier M, Durand P (1986) REGULAR 2-COMPONENT PAULI-LIKE EFFECTIVE-HAMILTONIANS IN DIRAC THEORY. Phys Scr 34:394–404
98. Heully JL, Lindgren I, Lindroth E, Lundqvist S, Martensson-pendrill AM (1986) DIAGONALIZATION OF THE DIRAC HAMILTONIAN AS A BASIS FOR A RELATIVISTIC MANY-BODY PROCEDURE. J Phys B 19:2799–2815
99. van Lenthe E, Baerends EJ, Snijders JG (1993) RELATIVISTIC REGULAR 2-COMPONENT HAMILTONIANS. J Chem Phys 99:4597–4610
100. van Lenthe E, Baerends EJ, Snijders JG (1994) Relativistic total-energy using regular approximations. 101:9783–9792
101. van Lenthe E (1996) The ZORA equation. Vrije Universiteit Amsterdam, Amsterdam, Netherlands
102. Filatov M, Cremer D (2003) On the physical meaning of the ZORA Hamiltonian. Mol Phys 101:2295–2302
103. Anderson JSM, Rodriguez JI, Ayers PW, Gotz AW (2017) Relativistic (SR-ZORA) Quantum Theory of Atoms in Molecules properties. J Comput Chem 38:81–86
104. Wang LL, Ping Y, Momen R, Azizi A, Xu TL, Rodriguez JI, Anderson JSM, Kirk SR, Jenkins S (2017) Insights into the all-metal Sb3Au3Sb3 (3) sandwich complex from a QTAIM and stress tensor analysis. Chem Phys Lett 685:127–132
105. Anderson JSM, Rodriguez JI, Ayers PW, Trujillo-Gonzalez DE, Gotz AW, Autschbach J, Castillo-Alvarado FL, Yamashita K (2019) Molecular QTAIM Topology Is Sensitive to Relativistic Corrections. Chem -Eur J 25:2538–2544
106. Marwitz AJV, Matus MH, Zakharov LN, Dixon DA, Liu S-Y (2009) A Hybrid Organic/Inorganic Benzene. Angew Chem Int Ed 48:973–977
107. Dewar MJS, Kubba VP, Pettit R (1958) New heteroaromatic compounds. Part I. 9-Aza-10-boraphenanthrene. RSC 624 3073–3076
108. Dewar MJS (1989) A critique of frontier orbital theory. THEOCHEM 59:301–323
109. Anderson JSM, Melin J, Ayers PW (2007) Conceptual density-functional theory for general chemical reactions, including those that are neither charge- nor frontier-orbital-controlled. 2. Application to molecules where frontier molecular orbital theory fails. J Chem Theory Comput 3:375–389
110. Anderson JSM, Melin J, Ayers PW (2007) Conceptual density-functional theory for general chemical reactions, including those that are neither charge nor frontier-orbital controlled. I. Theory and derivation of a general-purpose reactivity indicator. J Chem Theory Comput 3:358–374
111. Anderson JSM, Ayers PW (2007) Predicting the reactivity of ambidentate nucleophiles and electrophiles using a single, general-purpose, reactivity indicator. Phys Chem Chem Phys 9:2371–2378
112. Anderson JSM, Liu YL, Thomson JW, Ayers PW (2010) Predicting the quality of leaving groups in organic chemistry: Tests against experimental data. J Mol Struct THEOCHEM 943:168–177
113. Anderson JSM, Melin J, Ayers PW (2016) Using the general-purpose reactivity indicator: challenging examples. J Mol Model 22
114. Barrera Y, Rocha-Rinza T, Mulks FF, Ayers PW, Anderson JSM (2025) The Grand Canonical General-Purpose Reactivity Indicator: A Conceptual DFT Approach to Predict Molecular Reactivity and Experimental Electrophilicity and Nucleophilicity Scales. J Chem Theory Comput 21:12508–12522
115. Anderson JSM, Ayers PW (2014) Resolving the nature of the reactive sites of phenylsulfinate (PhSO2-) with a single general-purpose reactivity indicator. Comput Theor Chem 1043:1–4

116. Contreras-Torres FF, Basiuk VA, Basiuk EV (2008) Regioselectivity in Azahydro[60]fullerene Derivatives: Application of General-Purpose Reactivity Indicators. J Phys Chem A 112:8154–8163
117. Wang H, Dong W, Shi J (2023) Theoretical speculation on the chemical reaction activity site and degradation mechanism of chloramphenicol. Chem Phys Lett 811:140195
118. Ayers PW, Anderson JSM, Bartolotti LJ (2005) Perturbative perspectives on the chemical reaction prediction problem. Int J Quantum Chem 101:520–534
119. Ureiro-Cueto G, Anderson JSM (2025) Exploration of the eigenvectors of the Localization Delocalization Matrices for TiO2 Finite Cells and Solids: From resonance to QTAIM. Submitted to Structural Chemistry Special Issue. From Fundamentals to Applications, Electron Localization and Delocalization
120. Ayers PW (2005) Electron localization functions and local measures of the covariance. J Chem Sci 117:441–454
121. Yuen K-V (ed) (2010) (eds) Bayesian Methods for Structural Dynamics and Civil Engineering. Wiley & Sons Asia, Singapore
122. Thacker WC (1989) The role of the Hessian matrix in fitting models to measurements. J Geophys Res Oceans 94:6177–6196
123. Shir OM, Yehudayoff A (2020) On the covariance-Hessian relation in evolution strategies. Theor Comput Sci 801:157–174